Journal of Statistics & Management Systems
ISSN 0972-0510 (Print), ISSN 2169-0014 (Online)
Vol. 27 (2024), No. 8, pp. 1525–1539
DOI : 10.47974/JSMS-1011

Age-structured model with varied contact patterns and vaccination of COVID-19 in Liaoning Province, China

Tengxin He [#]
Ning Lia *
Department of Mathematics
College of Sciences
Northeastern University
Shenyang 110819
Liaoning
China

Abstract

Measuring age heterogeneity and the role of vaccines in the epidemic, an age-structured SVEIHR model is developed to simulate the propagation of the third outbreak of COVID-19 in Liaoning Province. Based on the actual data, parameters are obtained by the MCMC method and used in numerical analysis and the calculation of the basic reproduction number for different contact patterns and vaccine efficacy. The appropriate method of epidemic management obtained in this paper is to conduct self-quarantine first, and then resume work under the management policy, which can productively halt the epidemic. Besides, it is found that vaccination can effectively alleviate the epidemic situation. Specifically, the more effective the vaccine is, the fewer people will become infected.

Subject Classification: *93C15, 92B05.*

Keywords: *COVID-19, Age-structured, Contact patterns, Vaccination.*

1. Introduction

Since the end of 2019, Corona Virus Disease 2019 (COVID-19), a novel coronavirus pneumonia, has had a significant impact on people's health and lives, as COVID-19 is highly contagious and generally susceptible, primarily transmitted through droplet respiratory particles, direct contact, and aerosol propagation. In order to investigate the transmission of

---

[#] *E-mail:* **20201793@stu.neu.edu.cn**
* *E-mail:* **lining80@163.com (Corresponding Auhor)**

COVID-19 and analyze the pivotal factors of its epidemic, a representative dynamic model, the SEIR model, is extensively used and improved while taking into account various aspects ranging from quarantined to media coverage [1, 2, 3]. And the vaccine factor is no exception. Kar et al. [4] used the SIR model and regarded the vaccine as a way to turn susceptible people into removed people. Shen et al. [5] adjusted the SEIAHR model by appending a new compartment for vaccinated individual and compared the number of averted infections under different policies to demonstrate the effectiveness of the vaccine.

However, vaccine is age-heterogeneous. It's unrealistic to simply summarize people into a same situation. That's why the initial vaccination in China was exclusively for people aged 18-59, and until July 2021, people aged 3-17 were permitted to be vaccinated. Accordingly, Choi et al. [6] used age-structured model to simulate and analyze vaccine priority policy. Additionally, an age-structured model can be employed in conjunction with a contact matrix to measure various contact patterns. The basic reproduction number and contact matrix were used by Zhang et al. [7] to measure the changes in four places before and after the relaxing strategy. Wang et al. [8] compared community-mode and house-mode contact patterns with an age-structured SEIHR model in Guangdong province.

China's vaccination is world-ahead of the curve. As of January 2, 2022, China had 132479 confirmed cases, which is a small quantity compared to the rest of the world. As early as January 15, 2021, China began the first batch of vaccinations, and more than 2 billion 847 million doses have been administered to date [9]. Furthermore, China's vaccination benefits the entire world. For instance, by the end of 2021, China's new inactivated vaccine had been approved for marketing in the UAE, with an efficacy of about 86%.

There is currently no associated research on mathematical modeling of COVID-19 transmission in Liaoning, China. In Liaoning province, as of February 7, 2022, the infection of COVID-19 is mostly concentrated in Shenyang and Dalian, particularly Dalian. Three outbreaks occurred in Dalian in mid-2020, late 2020, and late 2021. In the latest outbreak, the third outbreak, the first case was confirmed on November 4, 2021, who worked in cold storage [10]. Combined with the information disclosed by the Health Commissions and the People's Government of each city, the ages of patients without stated age are estimated in combination with action track and occupation description, and the daily new cases of each age group during the third outbreak are obtained, as shown in Figure 1.

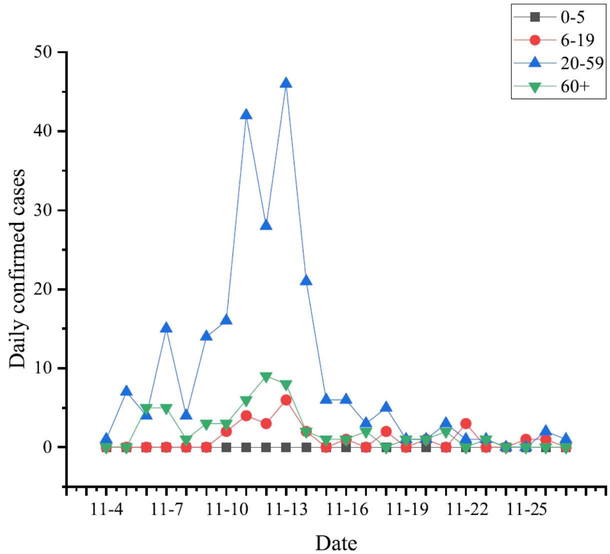

Figure 1

Daily confirmed cases in Liaoning province

From Figure 1, we can see that age heterogeneity is significant in the transmission process of the epidemic in that the number of new infections every day varies according to age group. So we considered using an age-structured model for the description, which can well reflect the distinct infection rate and interactions among different age groups. In addition, in order to assess the effectiveness of the vaccination, we established a new compartment for vaccinated people in differential equations. So in this study, we used an age-structured SVEIHR model to fit the third epidemic in Liaoning Province. Using the parameters provided by fitting, numerical analysis and basic reproduction numbers were used to analyze the impact of different contact patterns and vaccine efficacy on the epidemic. Thus, we have obtained a better management measure and the conclusion that higher vaccine efficacy results in better mitigation of the epidemic.

The remainder of the paper is structured as follows. Section 2 establishes the age-structured SEVIHR model and calculates the basic reproduction number. Section 3 contains the parameter estimation. Section 4 evaluates the factor of contact patterns and vaccination and Section 5 provides the discussion and conclusion.

2. Model Formulation

To describe the transmission of COVID-19 in Liaoning, combining age heterogeneity and vaccine factors, we extended SEIR model to an age-structured SVEIHR model. We hypothesized that births and natural deaths had no influence on the dynamics because of COVID-19's rapid dissemination and the short time span in this study. The population was separated into four age groups in this model. Individuals aged 0-5, 6-19, 20-59, and 60+ are represented by the classes $i = 1,2,3,4$, and people in each class (N) are divided into Susceptible (S), Exposed (E), Vaccinated (V), Infectious (I), Hospitalized (H) and Recovered (R). The epidemiological dynamics of the model are depicted in Figure 2.

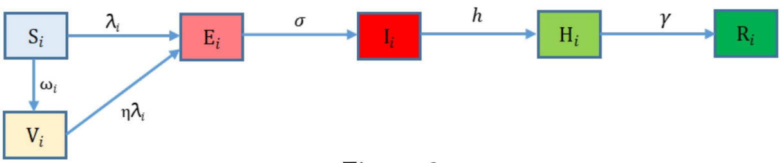

Figure 2

COVID-19 transmission model flowchart

If an infectious individual comes into contact with a susceptible or vaccinated person, the infection can occur. In each age group, the transmission rate owing to effective contact of S with I is given as $\lambda_i = \beta_i \sum_{j=1}^{4} c_{ij} \frac{I_j(t)}{N_j(t)}$, where β_i is the infection probability of a person in age group i per contact and c_{ij} represents the average number of contacts between individuals in age group i and individuals in age group j. $1-\eta$ denoted the vaccine efficacy in preventing infection, while the infection probability for a vaccinated person is represented by η. ω_i is the daily doses of vaccination. $1/\sigma$ is the incubation period. h stands for the hospitalization rate among infectious individuals and $1/\gamma$ is the recovery period. The dynamic model was defined by the following differential equations based on the assumptions stated above.

$$\begin{cases} S_i'(t) = -\lambda_i S_i(t) - \omega_i S_i(t) \\ V_i'(t) = \omega_i S_i(t) - \eta\lambda_i \ V_i(t) \\ E_i'(t) = \lambda_i S_i(t) + \eta\lambda_i \ V_i(t) - \sigma E_i(t) \\ I_i'(t) = \sigma E_i(t) - h I_i(t) \\ H_i'(t) = h I_i(t) - \gamma H_i(t) \\ R_i'(t) = \gamma H_i(t) \end{cases} \tag{1}$$

with initial conditions

$$S_i(0) = S_{i_0} \geq 0, V_i(0) = V_{i_0} \geq 0, E_i(0) = E_{i_0} \geq 0,$$

$$I_i(0) = I_{i_0} \geq 0, H_i(0) = H_{i_0} \geq 0, R_i(0) = R_{i_0} \geq 0. \ (i = 1,2,3,4)$$

The equation $\mathbf{N}_i'(t) = 0,$ specifically, the overall number of people in each age-group remains constant. So the feasible region

$$\Omega = \{(S_i, V_i, E_i, I_i, H_i, R_i) \in R_+^6 (i = 1,2,3,4) : 0 \leq S_i, V_i, E_i, I_i, H_i, R_i \leq N_i\}$$

is positive invariant.

The basic reproduction number R_0 represents the average number of new infections induced directly by an infected individual in a population of all susceptible people. Using next-generation matrix [11] we can obtain $F = \begin{pmatrix} 0 & F_1 \\ 0 & 0 \end{pmatrix}$ where

$$F_1 = \begin{pmatrix} \beta_1 c_{11} \frac{S_1+\eta V_1}{N_1} & \beta_1 c_{12} \frac{S_1+\eta V_1}{N_2} & \beta_1 c_{13} \frac{S_1+\eta V_1}{N_3} & \beta_1 c_{14} \frac{S_1+\eta V_1}{N_4} \\ \beta_2 c_{21} \frac{S_2+\eta V_2}{N_1} & \beta_2 c_{22} \frac{S_2+\eta V_2}{N_2} & \beta_2 c_{23} \frac{S_2+\eta V_2}{N_3} & \beta_2 c_{24} \frac{S_2+\eta V_2}{N_4} \\ \beta_3 c_{31} \frac{S_3+\eta V_3}{N_1} & \beta_3 c_{32} \frac{S_3+\eta V_3}{N_2} & \beta_3 c_{33} \frac{S_3+\eta V_3}{N_3} & \beta_3 c_{34} \frac{S_3+\eta V_3}{N_4} \\ \beta_4 c_{41} \frac{S_4+\eta V_4}{N_1} & \beta_4 c_{42} \frac{S_4+\eta V_4}{N_2} & \beta_4 c_{43} \frac{S_4+\eta V_4}{N_3} & \beta_4 c_{44} \frac{S_4+\eta V_4}{N_4} \end{pmatrix}$$

and $V = \begin{pmatrix} \sigma I_4 & O_{4\times4} \\ -\sigma I_4 & h I_4 \end{pmatrix},$ where I_4 is the identity matrix and $O_{4\times4}$ is the 4x4 zero matrix. Thus

$$R_0 = \frac{1}{h} \rho(F_1) \tag{2}$$

and $\rho(F_1)$ means the spectral radius of matrix F_1.

Theorem 2.1: *For system* (1), *there is a disease-free equilibrium*

$$E_0 = (0, N_1, 0,0,0,0, \cdots, 0, N_4, 0,0,0,0),$$

which is asymptotically stable if $R_0 < 1$ *and* F_1 *is irreducible.*

***Proof*:** By substituting the point E_0 into the equations (1), it can be obtained that the results at the right end of each equation are 0. That is, E_0 is the equilibrium point of the system.

Using the Perron-Frobenius theorem [12], there exists a positive left eigenvector $\omega = (\omega_1, \omega_2, \omega_3, \omega_4)$ of F_1, which satisfies the equation $\omega F_1 = \rho(F_1)$. Define the Lyapunov function

$$L(t)=\sum_{k=1}^{4}\omega_k(E_k(t)+I_k(t)).$$

Differentiating along the solutions of system (1) yields.

$$\begin{aligned}\frac{\mathrm{d}L(t)}{\mathrm{d}t}&=\sum_{k=1}^{4}\omega_k(\lambda_k(S_k(t)+\eta\mathrm{V}_k(t))-h\mathrm{I}_k(t))\\&=\sum_{k=1}^{4}\omega_k\left(\beta_k\sum_{j=1}^{4}c_{kj}\frac{\mathrm{I}_j(t)}{\mathrm{N}_j(t)}(S_k(t)+\eta\mathrm{V}_k(t))-h\mathrm{I}_k(t)\right)\\&=h\omega\left(\frac{1}{h}F_1-I_4\right)\boldsymbol{I}=h(R_0-1)\omega\boldsymbol{I}\end{aligned}$$

where $\boldsymbol{I}=(I_1,I_2,I_3,I_4)^T$. When $R_0<1$, we have $\frac{\mathrm{d}L(t)}{\mathrm{d}t}\le 0$ and $\frac{\mathrm{d}L(t)}{\mathrm{d}t}=0$ if and only if $\boldsymbol{I}=0$, so the largest compact invariant set $\{L'(t)=0\}$ is the singleton $\{E_0\}$. Using the LaSalle invariant principle [13], the disease equilibrium point E_0 is globally asymptotically stable.

Infectious diseases will be managed if R_0 is kept below one, according to Theorem 2.1. As a result, from a different perspective, the aim to implementing various strategies is to minimize R_0.

Taking the parameters obtained in Section 3 as an example, the effects of various parameters of the model on the basic reproduction number are analyzed by using partial rank correlation coefficients (PRCCs) [14]. As shown in Figure 3, reducing the infection rate, improving the vaccine efficacy and increasing the proportion of vaccinated people can well reduce the basic reproduction number. Among them, the most significant variables for the basic reproduction number are vaccine efficacy and the infection rate of the 6-19 and 20-59 age groups, which are the key factors in the control of epidemics.

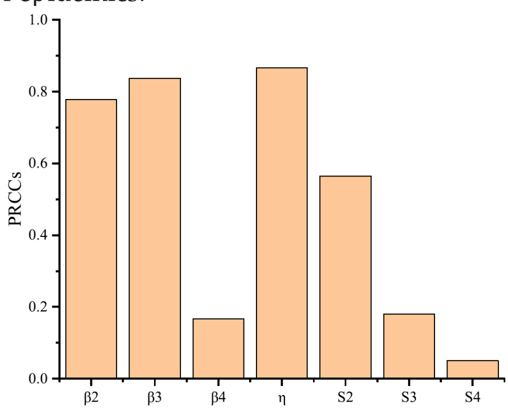

Figure 3

Sensitivity analysis of the basic reproduction number

3. Parameters Estimation

3.1 *Data Source*

The Health Commission of Liaoning Province [15] provided the majority of the data on COVID-19 infected people in Liaoning from November 3 to November 29, 2021. The data collection comprises the total number of discovered infected cases, newly discovered infected cases, and recovered cases and the specific data of each age group is obtained the Health Commission of each city. Further, The statistics fitted in this research are those that have been published or can be extrapolated. The population data were obtained from the seventh census bulletin and the annual birth rate of Liaoning Province [16].

Value of vaccination efficacy, incubation period and recovery rate are received from different sources, which are displayed in Table 1. Besides, as shown in Figure 4, the contact pattern is described by the contact matrix [17], which is divided into four modes: community, home, workplace and school.

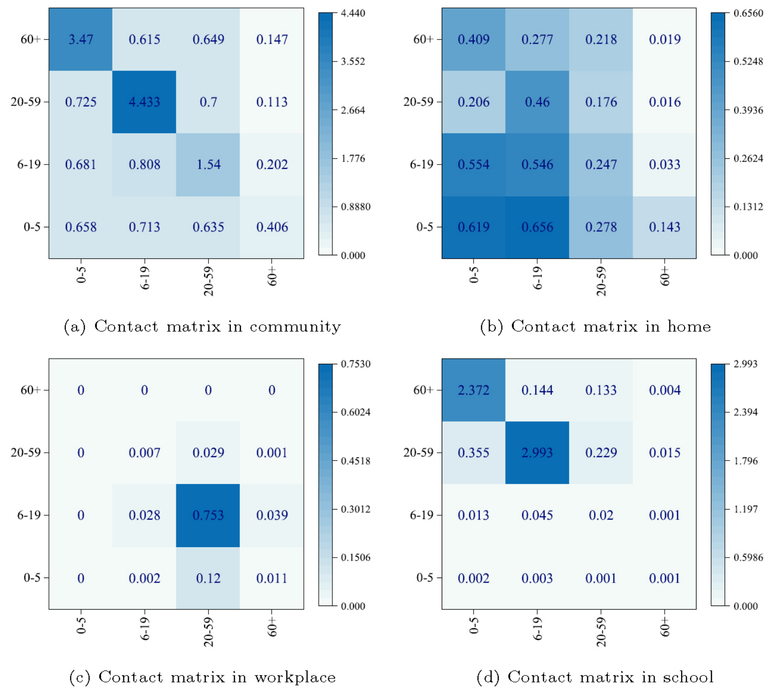

(a) Contact matrix in community

(b) Contact matrix in home

(c) Contact matrix in workplace

(d) Contact matrix in school

Figure 4

Contact matrix under diverse contact patterns [17]

3.2 *Parameters Estimation*

According to the study in [6], the vaccine efficacy is around 0.88. We obtained that average incubation is 5 days from paper [18]. Furthermore, as shown in the article [19], the average treatment time is 10 days.

During the third outbreak, there are no newly infected children aged 0 to 5. As a result, we solely utilized data from the other three age groups to simulate and estimate their infection probability. We derived parameter values and 95% confidence intervals (95% CI) using the Markov Chain Monte Carlo (MCMC) method with the Metropolis-Hasting algorithm [20], which are presented in Table 1.

Table 1

Description and values of parameters

Parameter	Description	Value	95%CI	Source
β_i	Infection probability of age group i	0.1438, 0.2371, 0.2015[1]	[0.1399, 0.1477], [0.2370, 0.2455], [0.1987, 0.2043]	Estimated
ω_i	Effective vaccination rate of age group i	0.024, 0.008, 0.006	[0.023, 0.025], [0.007, 0.009], [0.005, 0.007]	Estimated
$1-\eta$	Vaccine efficacy	0.88	-	[6]
$1/\sigma$	Incubation period	5	-	[18]
h	Hospitalization rate	0.340	[0.334, 0.346]	Estimated
$1/\gamma$	Recovery period	10	-	[19]

[1] All values involving subscript i in the table correspond to age group: 6-19, 20-59, 60+ respectively from left to right, namely $i = 2,3,4$

It can be noticed that the infection rate and vaccination rate of the 20–59 age group are relatively high, owing to the age group's large population. In comparison to the per capita infection rate, it is observed that the infection probability of COVID-19 in people over 60 is the highest.

Using the fitted parameter data, we can do a specific analysis of different variables and carry out numerical simulations in Section 4.

3.3 *Fitting Results*

Figure 5 illustrates the estimated cumulative infected cases and COVID-19 real data in different age groups. The simulations are relatively compatible with the reported cases, which verifies the validity of our model to some extent. The error is primarily due to the fact that this outbreak is concentrated in closed environments such as cold storage and schools, so the contact matrix of the community model cannot completely describe the contact relationship, and there is uncertainty about the age of the data. Furthermore, as seen in Figure 5, the later time fitting effect quite outperforms the earlier fitting effect. It might be due to a lag in data statistics during the early stages of the outbreak, which created a diversion from the true situation. So the error is considered to be within acceptable limits.

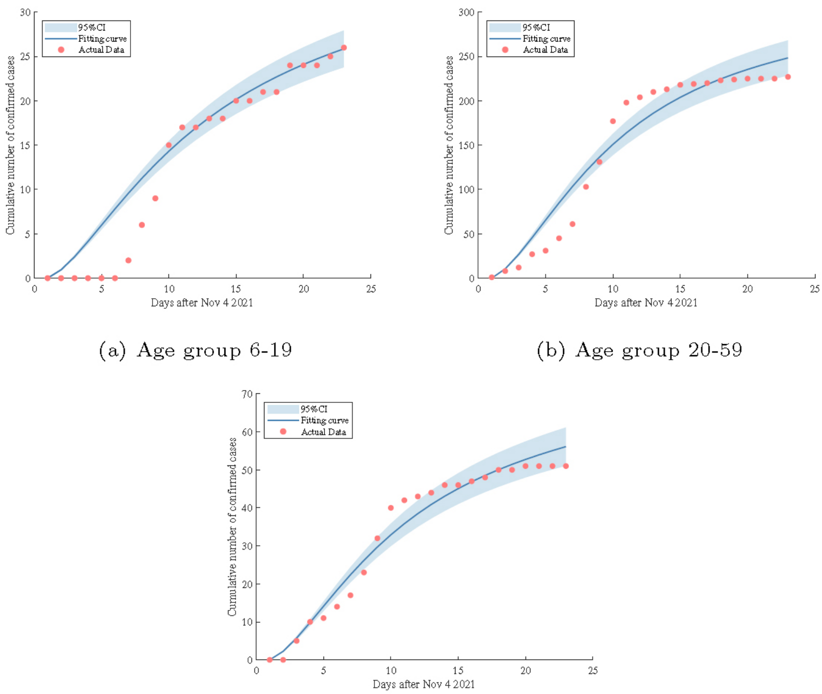

(a) Age group 6-19

(b) Age group 20-59

(c) Age group 60+

Figure 5

Fitting results of cumulative number of infected cases in Liaoning with its actual data of different age groups

4. Effects of contact patterns and vaccine efficacy

Figure 4 shows the specific values of various contact patterns. The combination of the school pattern and work pattern can be regarded as the community pattern under the control (controlled community pattern), and the home pattern is regarded as the self-quarantined pattern.

When the infection rate remains constant, it can be observed in Figure 6 that in the case of self-isolation, the peak number of new infections and the cumulative number decreases somewhat compared to the initial social contact pattern. Furthermore, the peak number and total number of infections in the controlled social contact pattern are significantly lower than the other two patterns.

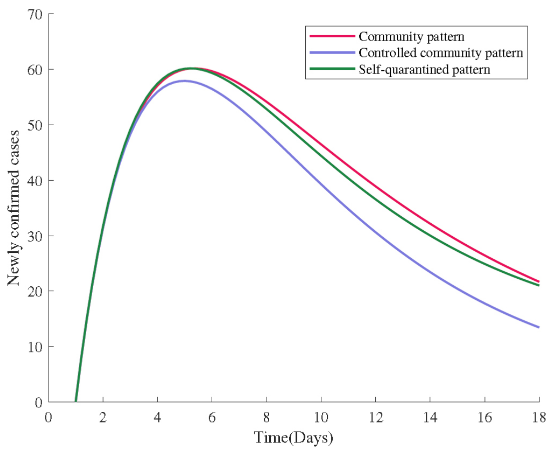

Figure 6

Simulation results for the number of newly confirmed cases with different contact patterns

η denotes the infection probability for a vaccinated person. Thus if a vaccine is more efficient in preventing COVID-19, the vaccinated individual is less likely to become infected. Figure 7 reflects the influence of different vaccine efficacy. It shows that when $\eta = 0$, that is, when the vaccinated individual is no different from the recovered person, the disease can be perfectly managed. When the infection rate among vaccinated persons is twice as high as it was previously, the peak and cumulative number of infected people will skyrocket. When the infection rate reaches three times, the number of daily infections increases constantly, and the epidemic becomes difficult to control.

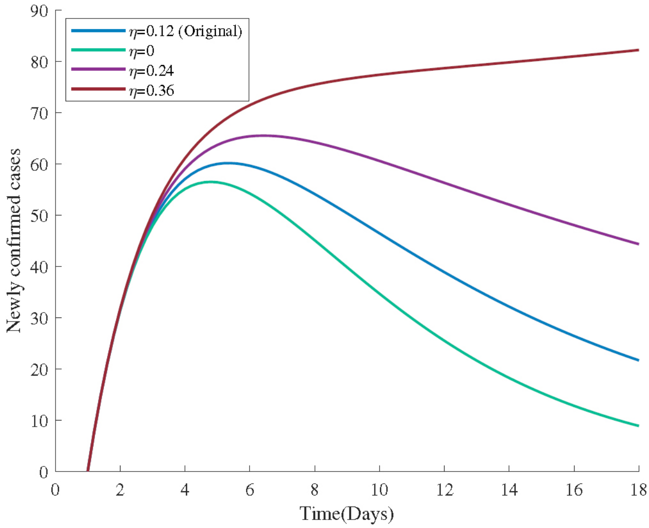

Figure 7

Simulation results for the number of newly confirmed cases with different vaccine efficacy

The influence of contact patterns and vaccines can also be shown by the basic reproduction number R_0 above. R_0 is a function of S and V, which change with time, so R_0 at their initial time is taken for comparison. The results are shown in Table 2 and Table 3.

Table 2

R_0 in initial time under different contact patterns

Contact Patterns	Community Pattern	Controlled Community Pattern	Self-Quarantined Pattern
R_0	0.2730	0.1683	0.0492

Table 3

R_0 in initial time under different vaccine efficacy

η	0	0.06	0.12	0.18	0.24	0.3
R_0	0.2141	0.2436	0.2730	0.3025	0.3320	0.3615

It can be seen that the size of the basic reproduction number is completely consistent with the above numerical analysis of vaccine efficacy. For the contact pattern, it shows that the self-quarantined pattern is more suitable for consideration in the early stages of the epidemic, and the community pattern under control is more suitable for the long-term plan.

5. Conclusion and Discussion

In this paper, we constructed an age-structured SEIHR model with vaccination to reflect the epidemic in Liaoning province, particularly the third outbreak. We gave the expression of the basic reproduction number and proved that when $R_0 < 1$, the infectious disease will disappear and tend to be stable. Moreover, We have used PRCCs for sensitivity analysis and provide the relationship between the parameters and the basic reproduction number. We used MCMC algorithm and obtained the important parameters in the epidemic, we found that the per capita prevalence rate of people over the age of 60 is relatively high, and further applied these parameters in numerical analysis. We have proved the effectiveness of self-quarantine pattern and management policy in epidemic prevention and control. In detail, self-isolation is more suitable for the early stage of epidemic management, and the resumption of work based on management policy is more suitable for the middle and late stages. We also proved the effectiveness of the vaccine. More specifically, the better the effect of the vaccine, the better the effect of epidemic prevention and control.

The importance of age heterogeneity should be emphasized, not only in the infection possibilities of different ages but also in the contact pattern. For instance, this epidemic in Liaoning mainly occurred in cold storage and schools, which are typical places with age representation. Besides, various age groups have distinct vaccination requirements and acceptability, which also have to be taken into consideration for policies.

From the perspective of specific policies, the best method recommended and proved in this paper is to quarantine for control at the beginning of the epidemic, and then return to work under the management of the government when the epidemic is gradually stable. This can effectively slow down the epidemic and continue the urban economy and the needs of the people.

Besides, it is very important to promote more effective vaccines. It can be seen from the study that if the vaccine effect has not reached a certain benefit, the disease will be difficult to control. Since $S+V$ is basically equal to the fixed value N, from the expression of the basic regeneration number, strengthening vaccination can effectively reduce the basic regeneration number and control the epidemic situation, which also verifies the importance of the vaccine barrier.

There are still many limitations to this paper. For example, when designing the model, we set the infection rate as a linear relationship, but in fact, the infection rate changes with the number of infected people and vaccinated people. Besides, there is no epidemic in this outbreak at the age of 0-5, and we have not fit into this age group. Many of our parameters and contact matrix are cited in the literature, which is still distant from reality to some extent. Moreover, the parameters such as vaccine efficiency and incubation period were not stratified by age. More data is needed to further prove it. We will leave this to the follow-up work.

References

[1] F. Li, Z. Jin, and J. Zhang, "Assessing the effectiveness of mass testing and quarantine in the spread of COVID-19 in Beijing and Xinjiang, 2020," *Complexity*, vol. 2021, art. no. 5510428 (2021).

[2] B. Tang, F. Xia, S. Tang, N. L. Bragazzi, Q. Li, X. Sun, J. Liang, Y. Xiao, and J. Wu, "The effectiveness of quarantine and isolation determine the trend of the COVID-19 epidemic in the final phase of the current outbreak in China," *International Journal of Infectious Diseases*, vol. 96, pp. 636-647 (2020).

[3] X. Chang, J. Wang, M. Liu, Z. Jin, and D. Han, "Study on an SIHRS model of COVID-19 pandemic with impulse and time delay under media coverage," *IEEE Access*, vol. 9, pp. 49387-49397 (2021).

[4] T. K. Kar and A. Batabyal, "Stability analysis and optimal control of an SIR epidemic model with vaccination," *Biosystems*, vol. 104, no. 2-3, pp. 127-135 (2011).

[5] M. Shen, J. Zu, C. K. Fairley, J. A. Pagan, L. An, Z. Du, Y. Guo, L. Rong, Y. Xiao, G. Zhuang, et al., "Projected COVID-19 epidemic in the United States in the context of the effectiveness of a potential vaccine and implications for social distancing and face mask use," *Vaccine*, vol. 39, no. 16, pp. 2295-2302 (2021).

[6] Y. Choi, J.-S. Kim, J.-E. Kim, H. Choi, and C.-H. Lee, "Vaccination prioritization strategies for COVID-19 in Korea: A mathematical modeling approach," *International Journal of Environmental Research and Public Health*, vol. 18, no. 8, art. no. 4240 (2021).

[7] J. Zhang, M. Litvinova, Y. Liang, W. Zheng, H. Shi, A. Vespignani, C. Viboud, M. Ajelli, and H. Yu, "The impact of relaxing interventions on human contact patterns and SARS-CoV-2 transmission in China," *Science Advances*, vol. 7, no. 19, art. no. eabe2584 (2021).

[8] G. Q. Wang, S. Zhang, J. Y. Yang, and X. K. Xu, "Study of coupling the age-structured contact patterns to the COVID-19 pandemic transmission," *Wuli Xuebao/Acta Physica Sinica*, vol. 70, no. 1, art. no. 010201 (2021).

[9] National Health Commission of the People's Republic of China, "Novel coronavirus vaccination situations," Beijing Times, Jan. 3 (2022). [Online]. Available: http://www.nhc.gov.cn/jkj/s7915/202201/48ae26522c1f449c93b17069ac989c2a.shtml.

[10] Xinmin Evening News, "The first outbreak in Dalian came from cold storage, which is the third outbreak due to the cold chain," Beijing Times, Nov. 15 (2021). [Online]. Available: https://baijiahao.baidu.com/s?id=1716442579963421002&wfr=spider&for=pc.

[11] P. Van den Driessche and J. Watmough, "Reproduction numbers and subthreshold endemic equilibria for compartmental models of disease transmission," *Mathematical Biosciences*, vol. 180, no. 1-2, pp. 29-48 (2002).

[12] R. A. Horn and C. R. Johnson, Matrix analysis, 2nd ed., Cambridge: Cambridge University Press (2012).

[13] J. P. La Salle, The stability of dynamical systems, Philadelphia: SIAM (1976).

[14] S. Marino, I. B. Hogue, C. J. Ray, and D. E. Kirschner, "A methodology for performing global uncertainty and sensitivity analysis in systems biology," *Journal of Theoretical Biology*, vol. 254, no. 1, pp. 178-196 (2008).

[15] Health Commission of Liaoning Province, "Epidemic situation of COVID-19 pneumonia in Liaoning Province from 0:00 to 24:00 on December 29, 2021," Beijing Times, Dec. 30 (2021). [Online]. Available: http://wsjk.ln.gov.cn/wst_zdzt/xxgzbd/yqtb/202112/t20211230_4483063.html.

[16] T. B. of Statistics of Liaoning Province, "Bulletin of the seventh national census of Liaoning Province [1] (no. 1)," Beijing Times, May 30 (2021). [Online]. Available: https://tjj.ln.gov.cn/tjj/tjxx/tjgb/rkpcgb/C58140EFCB544341BBCFF8263718CD93/index.shtml.

[17] K. Prem, K. V. Zandvoort, P. Klepac, R. M. Eggo, N. G. Davies, A. R. Centre for the Mathematical Modelling of Infectious Diseases COVID-19 Working Group, and M. Jit, "Projecting contact matrices in 177 geographical regions: an update and comparison with empirical data for the COVID-19 era," PLoS Computational Biology, vol. 17, no. 7, art. no. e1009098 (2021).

[18] W. Zhou, A. Wang, F. Xia, Y. Xiao, S. Tang, "Effects of media reporting on mitigating spread of COVID-19 in the early phase of the outbreak," Math. Biosci. Eng., vol. 17, no. 3, pp. 2693-2707 (2020).

[19] H. G. Hong, Y. Li, "Estimation of time-varying reproduction numbers underlying epidemiological processes: A new statistical tool for the COVID-19 pandemic," PLoS One, vol. 15, no. 7, art. no. e0236464 (2020).

[20] H. Haario, M. Laine, A. Mira, E. Saksman, "Dram: efficient adaptive MCMC," Statist. Comput., vol. 16, no. 4, pp. 339-354 (2006).

Received March, 2022

Revised July, 2022